University of Groningen

Synthesis and Evaluation of F-18-Enzalutamide, a New Radioligand for PET Imaging of Androgen Receptors

Farinha Antunes, Inês; Dost, Rutger; Hoving, Hilde D; van Waarde, Aren; Dierckx, Rudi A; Samplonius, Douwe F; Helfrich, Wijnand; Elsinga, Philip H; de Vries, Erik F; de Jong, Igle J

IMPORTANT NOTE: You are advised to consult the publisher's version (publisher's PDF) if you wish to cite from it. Please check the document version below.

Document Version
Final author's version (accepted by publisher, after peer review)

[Link to publication in University of Groningen/UMCG research database](#)

Citation for published version (APA):
Farinha Antunes, I., Dost, R., Hoving, H. D., van Waarde, A., Dierckx, R. A., Samplonius, D. F., Helfrich, W., Elsinga, P. H., de Vries, E. F., & de Jong, I. J. (2021). Synthesis and Evaluation of F-18-Enzalutamide, a New Radioligand for PET Imaging of Androgen Receptors: A Comparison with 16 beta-F-18-Fluoro-5 alpha-Dihydrotestosterone. *Journal of Nuclear Medicine*, *62*(2), 1140-1145. https://doi.org/10.2967/jnumed.120.253641

Synthesis and evaluation of ^{18}F-enzalutamide, a new radioligand for PET Imaging of Androgen Receptors: A comparison with 16β-^{18}F-fluoro-5α-dihydrotestosterone

Inês F. Antunes[1]*, Rutger J. Dost[2]*, Hilde D. Hoving[2], Aren van Waarde[1], Rudi A.J.O Dierckx[1], Douwe F. Samplonius[3], Wijnand Helfrich[3], Philip H. Elsinga[1], Erik F.J. de Vries[1] and Igle J. de Jong[2]

1. Dept. of Nuclear Medicine and Molecular Imaging, University Medical Center Groningen, University of Groningen, Groningen, The Netherlands

2. Dept. of Urology, University Medical Centre Groningen, University of Groningen, Groningen, The Netherlands

3. Surgical Research Laboratory, University Medical Centre Groningen, University of Groningen, Groningen, The Netherlands

*Both authors contributed equally to this work

Corresponding author:

Dr. Inês F. Antunes

Department of Nuclear Medicine and Molecular Imaging, University Medical Center Groningen,

University of Groningen, PO Box 30.001, 9700 RB Groningen, The Netherlands, Tel.: +31-50-3610760,

FAX: +31-50-3611687, Email: i.farinha.antunes@umcg.nl

Running title: ^{18}F-enzalutamide for androgen-expression

Word count: 4616

ABSTRACT

Aim: 16β-18F-fluoro-5α-dihydrotestosterone (^{18}F-FDHT) is a radiopharmaceutical that has been investigated as a diagnostic agent for the assessment of androgen receptor (AR) density in prostate cancer using positron emission tomography (PET). However, ^{18}F-FDHT is rapidly metabolized in humans and excreted via the kidneys into the urine, which can compromise the detection of tumor lesions close to the prostate. Enzalutamide is an AR signaling inhibitor currently used in different stages of prostate cancer. Enzalutamide and its primary metabolite N-desmethyl enzalutamide have comparable affinity for the AR as FDHT but are both mainly excreted via the hepatic route. Radiolabeled enzalutamide could thus be a suitable candidate PET tracer for AR imaging. Here we describe the radiolabeling of enzalutamide with fluorine-18. Moreover, the in-vitro and in-vivo behavior of ^{18}F-enzalutamide was evaluated and compared to the current standard ^{18}F-FDHT.

Methods: ^{18}F-enzalutamide was obtained by the fluorination of this nitro precursor. In-vitro cellular uptake studies with ^{18}F-enzalutamide and ^{18}F-FDHT were performed in LNCaP (AR+) and HEK293 (AR-) cells. Competition assays with both tracers were conducted in the LNCaP (AR+) cell line. In-vivo PET imaging, ex-vivo biodistribution, and metabolite studies with ^{18}F-enzalutamide and ^{18}F-FDHT were conducted in athymic nude male mice bearing an LNCaP xenograft in the shoulder.

Results: ^{18}F-enzalutamide was obtained in 1.4±0.9% radiochemical yield with an apparent molar activity of 6.2±10.3 GBq/µmol. ^{18}F-FDHT was obtained in 1.5±0.8% yield with a molar activity > 25 GBq/µmol. Co-incubation with an excess of DHT or enzalutamide significantly reduced the cellular uptake of ^{18}F-enzalutamide and ^{18}F-FDHT to about 50% in AR+ LNCaP cells, but not in AR- HEK293 cells. PET and biodistribution studies in male mice bearing a LnCaP xenograft showed about 3 times higher tumor uptake for ^{18}F-enzalutamide than for ^{18}F-FDHT. Sixty minutes after tracer injection, 93% of ^{18}F-enzalutamide in plasma was still intact, compared to only 3% for ^{18}F-FDHT.

Conclusion: Despite its lower apparent molar activity, ^{18}F-enzalutamide shows higher tumor uptake and better metabolic stability than ^{18}F-FDHT and thus seems to have more favorable properties for imaging of AR with PET. However, further evaluation in other oncological animal models and patients is warranted to confirm these results.

INTRODUCTION

Prostate cancer has an incidence of 1.4 million per year, making it the leading cause of cancer for men (*1*). Prostate cancer is hormone-sensitive cancer that usually expresses androgen receptors, which play a prominent role in the development and treatment of the disease (*2*). The cornerstone of treatment has been androgen deprivation therapy or, if unsuccessful, chemotherapy (*2,3*). In more recent years, other hormonal therapies that focus on inhibition of androgen receptor-mediated signaling, such as the androgen receptor antagonist enzalutamide have been developed (*4*). For diagnosis and staging of prostate cancer, various imaging modalities are used to determine the extent of the disease. In general, a bone scan is performed to determine whether osseous metastases are present. For detection of lymph node or visceral metastases, PET and/or CT can be performed. For hormonal treatment to be successful, tumors must express the AR. AR expression can be determined on surgical or biopsy samples, but this would only give information about a small part of a single lesion. Since AR expression can be heterogeneous within and between lesions and can change over time, either spontaneously or as a result of treatment, whole body information about the AR status of all lesions in a patient would be advantageous. PET imaging with a suitable AR ligand as tracer could provide such information and would enable assessment of receptor occupancy of AR-targeting drugs. Such PET-CT methods for imaging of androgen receptor availability could not only be used to depict the extent of the disease but also to identify patients that would benefit from an AR targeting therapy and to monitor the efficacy of treatment. ^{18}F-Fluoro-dihydrotestosterone (^{18}F-FDHT) is a radiolabeled analog of 5α-dihydrotestosterone (DHT) and developed as a PET tracer for AR imaging (*5–10*). ^{18}F-FDHT shows high specific binding to the AR but is rapidly metabolized in humans (*6*). The circulating radiolabeled metabolites bind tightly to plasma proteins, leading to high background activity in blood and low contrast images. Moreover, ^{18}F-FDHT metabolites are cleared from the circulation via the kidneys into the urine, which can compromise the detection of tumor lesions close to the prostate. For these reasons, PET tracers for AR imaging with a different excretion route are required.

Unlike FDHT, enzalutamide is a pure AR antagonist that possesses a similar affinity towards AR as DHT and is currently used in androgen therapy (*11,12*). It is known that enzalutamide mainly metabolizes to N-desmethyl-enzalutamide which has a similar affinity towards AR as the parent compound (*13,14*). Besides, enzalutamide and N-desmethyl enzalutamide are primarily excreted via the hepatic route, which would result in low uptake in the kidneys and urine.

In this study, we, therefore, labeled enzalutamide with ^{18}F and investigated its potential as a PET tracer for AR imaging (Fig.1). For this purpose, we performed *in-vitro* and *in-vivo* studies in a prostate cancer cell line and castrated and uncastrated mice bearing AR-expressing tumor xenografts. The performance of ^{18}F-enzalutamide was compared to that of the currently applied tracer ^{18}F-FDHT (Fig.2).

MATERIAL AND METHODS

FDHT was purchased from PharmaSynth AS (Purity ≥95%) and enzalutamide was provided by Astellas. For radiolabeled compounds, the detection on the TLC was performed with Cyclone phosphor storage screens (multisensitive, Packard). These screens were exposed to the TLC strips for a few seconds and subsequently read out using a Cyclone phosphor storage imager (PerkinElmer) and analyzed with OptiQuant software. High-performance liquid chromatography (HPLC) purifications were performed with an Elite LaChrom VWR Hitachi L-2130 pump, using a Symmetry C18 HPLC column, connected to a UV-spectrometer (Elite LaChrom VWR Hitachi L-2400 UV detector) set at 254 nm and a Bicron frisk-tech radiation detector.

The synthesis and characterization of the nitro precursor (Supplemental Figure 1) as well as the in-vitro methods are presented in supplemental materials (available at http://jnm.snmjournals.org).

PET image reconstruction, data analysis and ex-vivo biodistribution were performed as previously described (*15*). Tracer uptake is expressed as %ID/g.

Radiosynthesis of ^{18}F-enzalutamide

Aqueous ^{18}F-fluoride was produced by irradiation of ^{18}O-water with a Scanditronix MC-17 cyclotron via the [18]O(p,n)[18]F nuclear reaction. The ^{18}F-fluoride solution was passed through a QMA SepPak Light anion exchange cartridge (Waters) to recover the ^{18}O-water. The ^{18}F-fluoride was eluted from the cartridge with 1 mL of $KHCO_3$ (1 mg/mL) and collected in a vial with 15 mg kryptofix[2.2.2]. To this solution, 1 mL acetonitrile was added and the solvents were evaporated at 130 °C. The ^{18}F-KF/kryptofix complex was dried 3 times by the addition of 0.5 mL acetonitrile, followed by evaporation of the solvent. ^{18}F-Enzalutamide was prepared by aromatic nucleophilic fluorination of the corresponding nitro precursor. Thus, the dried ^{18}F-KF/Kryptofix complex was dissolved in 0.5 mL of N,N-Dimethylformamide and added to compound **4** (2 mg, 4.01 μmol). The reaction mixture was heated at 150 °C for 30 min. After the mixture had cooled down, 0.5 mL of water was added. The product was purified by HPLC (eluent: 47% acetonitrile in water; flow: 4 mL/min; retention time: 14 min). The radioactive peak corresponding to the product was collected and diluted with 50 mL of distilled water and passed through an HLB Oasis cartridge (Waters, 30 mg). The product was eluted from the cartridge with 0.8 mL ethanol and diluted with 4.2 ml distilled water. Quality control was performed by UPLC, using a BEH Shield RP18 column (1.7 μm, 3.0x50 mm) and 40% aqueous acetonitrile as mobile phase at a flow of 1 mL/min.

Radiosynthesis of ^{18}F-FDHT

The fully automated synthesis of ^{18}F-FDHT was performed as previously described (*16*).

Animals

Athymic nude male mice (6-8 weeks old) were obtained from Harlan (Lelystad, The Netherlands). The animals were provided with standard laboratory chow and tap water *ad libitum*. All studies were carried out in compliance with the local ethical guidelines for animal experiments. The protocol was approved by the Institutional Animal Care and Use Committee (protocol number: DEC 6657D). After at least one week

of acclimatization, the mice were anesthetized and LNCaP cells [2 million cells in 100 µl of a 1:1 mixture of Matrigel and µl RPMI with 10 % fetal bovine serum] were subcutaneously injected into the neck/shoulder. Approximately 3 to 4 weeks after inoculation, tumor nodules were palpable.

Surgical Castration

One group of 7 mice were surgically castrated in the third week after tumor inoculation to reduce the levels of circulating androgens. Briefly, the animals where anesthetized using 2% isoflurane and placed on their back. Through a midline scrotal incision, the testes were ligated using Vicryl and the skin was closed using Vicryl Rapide, after which anesthesia was stopped. Perioperative analgesia was given subcutaneously using Finadyne 3 mg/kg. One animal developed a scrotal hematoma.

Pet Imaging in Xenograft Bearing Mice

Three to four weeks after LNCaP cell inoculation, the mice were anesthetized with 2% isoflurane, positioned in a transaxial position in the center of the field of view of the small animal PET camera (Focus 220, Siemens-Concorde). ^{18}F-enzalutamide (14±7 MBq) was mixed with either PBS (control) or enzalutamide (1mg/kg) in PBS and injected via the penile vein of the animal. ^{18}F-FDHT (9±4 MBq) was either mixed with PBS (control) or DHT (1mg/kg) in PBS before penile vein injection. Simultaneously with the injection of the PET tracer, an emission scan of 60 min was started. After the PET scan was complete, the animals were terminated with an overdose of anesthesia, and a 20-min transmission scan with a Co-57 point source was obtained for the correction of scatter and attenuation of 511 keV photons by tissue. After the transmission scan was completed, the animal remained fixed to the bed and the bed was positioned in the CT scanner (MicroCT II, CTI Siemens). A 15-min CT scan was acquired for anatomic localization of the tumor (exposure time=1050 msec; X-Ray voltage= 55 kvp; Anode current= 500 µA; number of rotation steps= 500; total rotation= 360 degrees).

Metabolite analysis

50 µL of acetonitrile was added to approximately 25 µL of plasma sample to precipitate the plasma proteins. The samples were centrifuged at 16,000g for 5 min. A 2 µL aliquot of the supernatant was collected and applied on a thin-layer chromatography plate. The thin-layer chromatography plate was eluted with n-hexane/ethyl acetate (1:4) (R_f ^{18}F-enzalutamide or ^{18}F-FDHT = 0.8, R_f metabolites=0.0). After elution, radioactivity on thin-layer chromatography plates was analyzed by phosphor storage imaging. Exposed screens were scanned with a Cyclone phosphor storage system (PerkinElmer) and the percentage of intact ^{18}F-enzalutamide or ^{18}F-FDHT as a function of tracer distribution time was calculated by region-of-interest analysis using OptiQuant Software.

Statistical Analysis

Statistical analyses were performed with Excel 2003 (Microsoft) and SigmaPlot (version 10.0; SPSS; Inc.). The IC_{50} values were calculated by fitting the data with non-linear regression using GraphPad Prism 5.0 (GraphPad software). Differences in tracer accumulation between groups were analyzed using the two-sided unpaired students´ t-test. Significance was reached when $p<0.05$. Throughout the manuscript, values are presented as mean $\pm$ SD.

RESULTS

Chemistry

The nitro precursor **4** was prepared through a four steps synthesis with an overall yield of 1.6% (supplementa figure 1) (*17,18*). The starting material, 2-nitro-4-bromobenzoic acid was transformed into methyl 2-(3-nitro-4-(methylcarbamoyl)phenylamino)-2-methylpropanoate **3** which was further reacted with 2-(trifluoromethyl)-4-isothiocyanatobenzonitrile to give the final precursor **4** in 35% yield.

Radiochemistry

^{18}F-enzalutamide was obtained in 1.4±0.9% radiochemical yield (decay corrected, based on ^{18}F-fluoride added to the precursor) within 98±8 min. At the end of synthesis, the apparent molar activity was 6.2±10.3 GBq/µmol and the radiochemical purity >95%. ^{18}F-FDHT was obtained in a 1.5±0.8% decay-corrected radiochemical yield. The molar activity of ^{18}F-FDHT was >25 GBq/µmol, with a radiochemical purity of >95%. ^{18}F-enzalutamide was stable for at least 60 min in the formulation solution, as no decomposition was observed by UPLC analysis. The distribution coefficients ($logD_{7.4}$) of ^{18}F-enzalutamide and ^{18}F-FDHT were 2.32±0.01 and 2.56±0.01, respectively.

In-vitro Binding Affinity

The human embryonic kidney HEK293 cell line is generally considered to be AR negative, whereas the LNCaP cells are AR-positive. In this study, this was confirmed by flow cytometry as depicted in the histograms in Fig. 3A, where HEK293 cells did not show any binding of the AR antibody while the LNCaP cells stained moderately with the AR antibody.

The *in-vitro* binding affinity of ^{18}F-enzalutamide and ^{18}F-FDHT towards AR was evaluated in AR-negative HEK293 and AR-positive LNCaP cells (Fig.3B, C). As expected, the uptake of ^{18}F-enzalutamide and ^{18}F-FDHT in HEK293 (AR-) could not be saturated with either DHT or enzalutamide. However, ^{18}F-enzalutamide and ^{18}F-FDHT uptake in LNCaP (AR+) was efficiently blocked with DHT or enzalutamide, suggesting both tracers selectively bind to AR. This selective binding to AR was further proven with a competitive displacement assay using either ^{18}F-enzalutamide or ^{18}F-FDHT and different concentrations of the competitive inhibitors: enzalutamide and DHT (Fig.4). Enzalutamide and DHT concentrations that inhibited 50% of tracer binding (IC_{50}) in LNCaP cells were 0.22 nM and 1.02 nM ^{18}F-enzalutamide and 1.72 nM and 4.07 nM for ^{18}F-FDHT, respectively.

In-vivo Pet Imaging

^{18}F-enzalutamide and ^{18}F-FDHT PET scans were performed in LNCaP tumor-bearing athymic nude mice that were injected with either vehicle or the AR ligands enzalutamide or DHT (Fig. 5). ^{18}F-enzalutamide PET scans were also performed in LNCaP tumor-bearing athymic nude mice that were castrated 3 weeks after tumor inoculation to reduce endogenous testosterone and DHT levels (Supplemental Fig.2). The time-activity curves of the tumors revealed slow kinetics for both PET tracers. The tracer accumulation in tumors obtained from the last 10 min of the PET scan (50-60 min) were 3.01±0.41 %ID/g (non-castrated) or 2.95±0.30 %ID/g (castrated) for ^{18}F-enzalutamide and 1.18±024 %ID/g (non-castrated) for ^{18}F-FDHT. Injection of ^{18}F-enzalutamide together with an excess of enzalutamide resulted in a significant reduction in tumor uptake (2.27±0.03 %ID/g, p<0.05, non-castrated). On the other hand, tumor uptake of ^{18}F-FDHT was significantly increased when co-injected with DHT (1.59±0.24 %ID/g, p<0.05, non-castrated).

Ex-vivo Biodistribution

Ex-vivo biodistribution of ^{18}F-enzalutamide and ^{18}F-FDHT was evaluated in the same animals that had received a PET scan. The results of the biodistribution and blocking experiments are depicted in table 1. In general, ^{18}F-enzalutamide exhibited significantly lower uptake in the liver, plasma and urine (p<0.001 for all) than ^{18}F-FDHT. In contrast, ^{18}F-enzalutamide exhibited significantly higher uptake in some androgen receptors expressing organs such as LNCaP xenografts, spleen, and brain, and similar uptake in small intestines, prostate, and bone (including bone marrow) when compared to ^{18}F-FDHT. When ^{18}F-enzalutamide was co-injected with enzalutamide, the uptake in the bone (containing bone marrow, p=0.0001), spleen (p=0.007), small intestines (p=0.03) and LNCaP xenograft (p=0.044) was significantly decreased by 68%, 59%, 56% and 37%, respectively. As for ^{18}F-FDHT, when co-injected with DHT the uptake was significantly decreased in the liver (p=0.001) and urine (p=0.025) and brown fat (p=0.047). The uptake of ^{18}F-enzalutamide was significantly higher in the prostate of castrated mice when compared to the uptake in non-castrated animals (p=0.008), but not in any of the other tissues.

Metabolite Analysis

Metabolite analysis revealed that only 3.1±2.1% (n=12) of the total plasma radioactivity consisted of intact ^{18}F-FDHT at 1h post-injection. ^{18}F-enzalutamide was more stable in vivo, as 93±14% (n=19) of the plasma activity at 1 h post-injection still consisted of the intact tracer.

DISCUSSION

This study shows that ^{18}F-enzalutamide appears to be a suitable PET tracer for imaging of AR expression in androgen-dependent tumors. As such, ^{18}F-enzalutamide could enable whole-body assessment of the stage of the disease, stratification of patients that could benefit from androgen therapy and evaluation of treatment efficacy. This study also showed that ^{18}F-enzalutamide seems to have better properties for imaging of AR expression in prostate cancer than the currently used PET tracer ^{18}F-FDHT.

The optimized radiolabeling of ^{18}F-enzalutamide consisted of a nucleophilic aromatic substitution reaction of the nitro analog of enzalutamide with ^{18}F-fluoride, leading to the desired product with similar yields as the labeling of ^{18}F-FDHT. Due to similar structures of the nitro-precursor and ^{18}F-enzalutamide, it was not possible to completely separate these two compounds by HPLC, leading to an apparent molar activity that was 4 times lower than that of ^{18}F-FDHT. Because of the structural similarity of the nitro-precursor with enzalutamide, it is reasonable to assume that the precursor also might have (some) affinity for the AR. Consequently, the contamination of ^{18}F-enzalutamide with precursor could have resulted in an underestimation of its binding properties for the AR, and thus its imaging performance.

To confirm that the ^{18}F-enzalutamide continues to possess a high affinity towards AR receptors, a competitive radiometric binding assay was performed with both tracers in LNCaP (AR-positive) and Hek293 (AR-negative) cells. Unlabeled enzalutamide and DHT were able to inhibit ^{18}F-enzalutamide and ^{18}F-FDHT binding in LNCaP cells, demonstrating that both ^{18}F-enzalutamide and ^{18}F-FDHT binding is AR-mediated. Competitive binding assays showed a similar binding affinity of ^{18}F-enzalutamide towards

the AR than ^{18}F-FDHT, despite the lower apparent molar affinity of the former tracer. The results of our binding assays are in agreement with data for the unlabeled drug reported in literature (*11*).

To evaluate the potential of ^{18}F-enzalutamide as a PET tracer for in-vivo imaging of AR expression, dynamic PET scans and ex-vivo biodistribution were performed in LNCaP tumor-bearing athymic nude male mice. First, we evaluated whether the castration of male mice would influence the uptake in the LNCaP xenografts. Ex-vivo biodistribution at 1h post tracer injection showed a similar distribution of ^{18}F-enzalutamide in castrated and non-castrated mice. Interestingly, only the uptake of ^{18}F-enzalutamide in the prostate was found to be significantly higher in castrated mice when compared to non-castrated, suggesting that the reduction of low circulating androgen levels increases the sensitivity of the tracer towards AR expressing organs by reducing the competition with the endogenous ligand. The castration-induced reduction in circulating androgen levels did not result in an increase in tracer uptake in the LNCaP xenograft (p=0.424), which could be due to the relatively high AR expression levels in LNCaP xenografts. In the case of high receptor expression, the effect of the occupancy of the receptor by the endogenous ligand is relatively small. To reduce the complexity of the experiment and animal discomfort, it was decided to demonstrate proof-of-principle of specific tracer uptake in LNCaP xenografts by performing the blocking studies with the AR ligands enzalutamide and DHT in non-castrated mice.

Despite both tracers having similar lipophilicities, they showed a somewhat different distribution pattern. ^{18}F-FDHT showed significantly higher accumulation in the liver, plasma, and urine than ^{18}F-enzalutamide. On the other hand, ^{18}F-enzalutamide had a significantly higher uptake in brown fat when compared to ^{18}F-FDHT. One of the reasons for these differences could be the difference in in-vivo stabilities. The metabolite analysis in the plasma indicated that ^{18}F-enzalutamide remained mostly intact during the time of the experiment (1h), whereas ^{18}F-FDHT was almost completely metabolized into less lipophilic compounds, which are likely excreted into the urine.

The time-activity curves of the tumors revealed slow kinetics for both PET tracers. However, the ^{18}F-enzalutamide accumulation in LNCaP tumors was about 3 times higher when compared to ^{18}F-FDHT. In

addition, the animals that were co-injected with an excess of unlabeled enzalutamide showed significantly lower tumor uptake of ^{18}F-enzalutamide, when compared to the ones that were co-injected with the vehicle. This result was confirmed by the results of the ex-vivo biodistribution suggesting that the tumor uptake of ^{18}F-enzalutamide is receptor-mediated. Such AR-mediated tumor uptake could not be demonstrated for ^{18}F-FDHT. Surprisingly, PET revealed that the uptake of ^{18}F-FDHT in the LNCaP xenograft was not reduced, but increased by co-injection with an excess of DHT. However, such an increase was not confirmed by the results of the ex-vivo biodistribution study, which did not reveal any difference in ^{18}F-FDHT uptake between DHT and vehicle-treated animals. The discrepancy between the PET and ex-vivo biodistribution results might be due to the difficulty in localizing the tumor in the PET images or a partial volume effect as a result of the small size of the tumors ($<0.1 cm^3$), potentially causing spill-over of background activity.

This proof-of-concept study has several limitations that need to be addressed. First, several mice did not develop LNCaP tumors and thus a relatively low number of animals remained for statistical analysis. Besides, the scans and the ex-vivo studies with ^{18}F-enzalutamide perhaps should have been extended to later time points since at 60 min tracer uptake is still increasing. Another limitation is the relatively low apparent molar activity of ^{18}F-enzalutamide, due to contamination with the precursor. Despite extensive optimization of the HPLC purification method, we were not able to completely remove the precursor from the product. Thus another synthesis routes should be investigated using a precursor that is easy to separate from the product. A possible solution could be to replace the nitro-precursor by the corresponding trimethylammonium precursor. Nonetheless, even with a low apparent molar activity ^{18}F-enzalutamide appeared to be a suitable PET tracer to image androgen receptors in tumors.

CONCLUSION

[18]F-enzalutamide can be readily radiolabeled with fluorine-18 with similar yields as ^{18}F-FDHT, although the apparent molar activity is relatively low. ^{18}F-enzalutamide is highly stable in-vivo and shows less

accumulation in the liver, plasma and urine, which is advantageous when evaluating local metastasis near the prostate. These promising preclinical results warrant further preclinical and clinical evaluation.

DISCLOSURE

ACKNOWLEDGMENTS

KEY POINTS

Question

Is the ^{18}F-Enzalutamde a more suitable PET tracer to access AR expression *in vivo*, compared to ^{18}F-FDHT?

Pertinent Findings

[18]F-enzalutamide shows higher tumor uptake, better metabolic stability and a lower plasma uptake than ^{18}F-FDHT in-vivo, and thus seems to have more favorable properties for imaging of AR with PET, originating images with higher contrast.

Implications For Patient Care

Since ^{18}F-Enzalutamide have the same structure as the AR signaling inhibitor (ARSi), this may enable a better understanding of ARSi-targeted drug development. Besides, by having more favorable properties as

a PET tracer it potentially may be used to more effectively select patients that would respond to such therapies and monitor the therapeutic effectiveness of these treatments.

REFERENCES

1.	Fitzmaurice C, Dicker D, Pain A, et al. The global burden of cancer 2013. *JAMA Oncol.* 2015;1:505.

2.	Shafi AA, Yen AE, Weigel NL. Androgen receptors in hormone-dependent and castration-resistant prostate cancer. *Pharmacol Ther.* 2013;140:223-238.

3.	Nader R, El Amm J, Aragon-Ching JB. Role of chemotherapy in prostate cancer. *Asian J Androl.* 20:221-229.

4.	Scott LJ. Enzalutamide: A Review in Castration-Resistant Prostate Cancer. *Drugs.* 2018;78:1913-1924.

5.	Larson SM, Morris M, Gunther I, et al. Tumor localization of 16beta-18F-fluoro-5alpha-dihydrotestosterone versus 18F-FDG in patients with progressive, metastatic prostate cancer. *J Nucl Med.* 2004;45:366-373.

6.	Beattie BJ, Smith-Jones PM, Jhanwar YS, et al. Pharmacokinetic Assessment of the Uptake of 16 -18F-Fluoro-5 -Dihydrotestosterone (FDHT) in Prostate Tumors as Measured by PET. *J Nucl Med.* 2010;51:183-192.

7.	Fox JJ, Gavane SC, Blanc-Autran E, et al. Positron Emission Tomography/Computed Tomography–Based Assessments of Androgen Receptor Expression and Glycolytic Activity as a Prognostic Biomarker for Metastatic Castration-Resistant Prostate Cancer. *JAMA Oncol.* 2018;4:217.

8.	Scher HI, Beer TM, Higano CS, et al. Antitumour activity of MDV3100 in castration-resistant prostate cancer: a phase 1–2 study. *Lancet.* 2010;375:1437-1446.

9.	Vargas HA, Kramer GM, Scott AM, et al. Reproducibility and Repeatability of Semiquantitative 18 F-Fluorodihydrotestosterone Uptake Metrics in Castration-Resistant Prostate Cancer Metastases: A Prospective Multicenter Study. *J Nucl Med.* 2018;59:1516-1523.

10.	Glaudemans AWJM, de Vries EFJ, Luurtsema G, et al. Detection of Intra-Abdominal Testicles with 16β-[18F]-Fluoro-5α-Dihydrotestosterone Positron Emission Tomography/Computed Tomography in a Pubertal Boy. *J Pediatr.* 2015;166:774-774.e1.

11.	Tran C, Ouk S, Clegg NJ, et al. Development of a Second-Generation Antiandrogen for Treatment of Advanced Prostate Cancer. *Science (80-).* 2009;324:787-790.

12.	Gauthier S, Martel C, Labrie F. Steroid derivatives as pure antagonists of the androgen receptor. *J Steroid Biochem Mol Biol.* 2012;132:93-104.

13.	Astellas. No Title. https://www.accessdata.fda.gov/drugsatfda_docs/label/2012/203415lbl.pdf. Published 2012.

14.	Kim T-H, Jeong J-W, Song J-H, et al. Pharmacokinetics of enzalutamide, an anti-prostate cancer drug, in rats. *Arch Pharm Res.* 2015;38:2076-2082.

15.	F Antunes I, Waarde A van, Dierckx RA, de Vries EGE, Hospers GAP, de Vries EF. Synthesis and Evaluation of the new Estrogen Receptor β selective radioligand [18F]FHNP: Comparison with

[18F]FES. *J Nucl Med*. 2017;58:554-559.

16.   Khayum MA, Doorduin J, Antunes IF, et al. In vivo imaging of brain androgen receptors in rats: a [18F]FDHT PET study. *Nucl Med Biol*. 2015;42:561-569.

17.   Jung ME, Ouk S, Yoo D, et al. Structure−Activity Relationship for Thiohydantoin Androgen Receptor Antagonists for Castration-Resistant Prostate Cancer (CRPC). *J Med Chem*. 2010;53:2779-2796.

18.   Jain, RP; Angelaud, R;Thompson, A et al. Processes for the synthesis of diarylthiohydantoin compounds. *WO2011106570 A1*. 2011.

FIGURES&TABLES
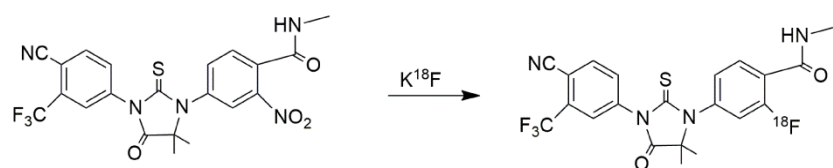
Figure 1. Scheme of the radiosynthesis of ^{18}F-enzalutamide.
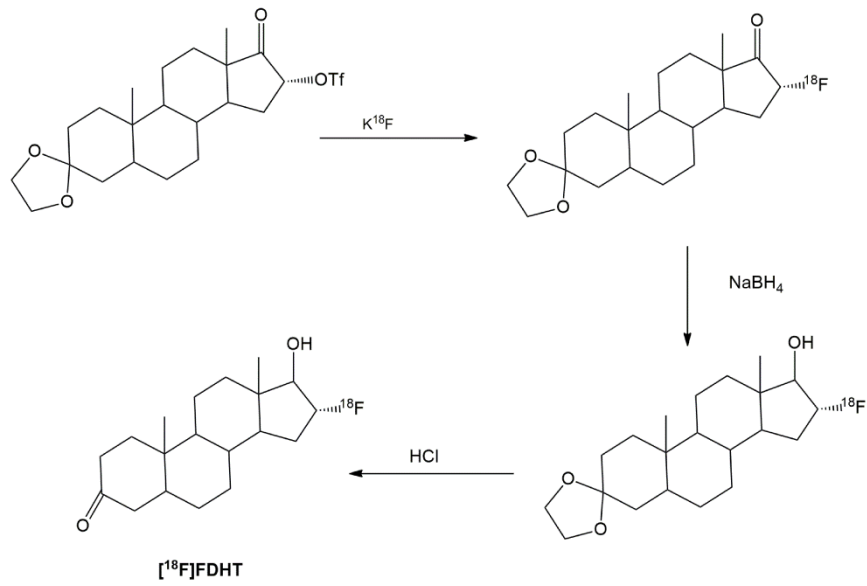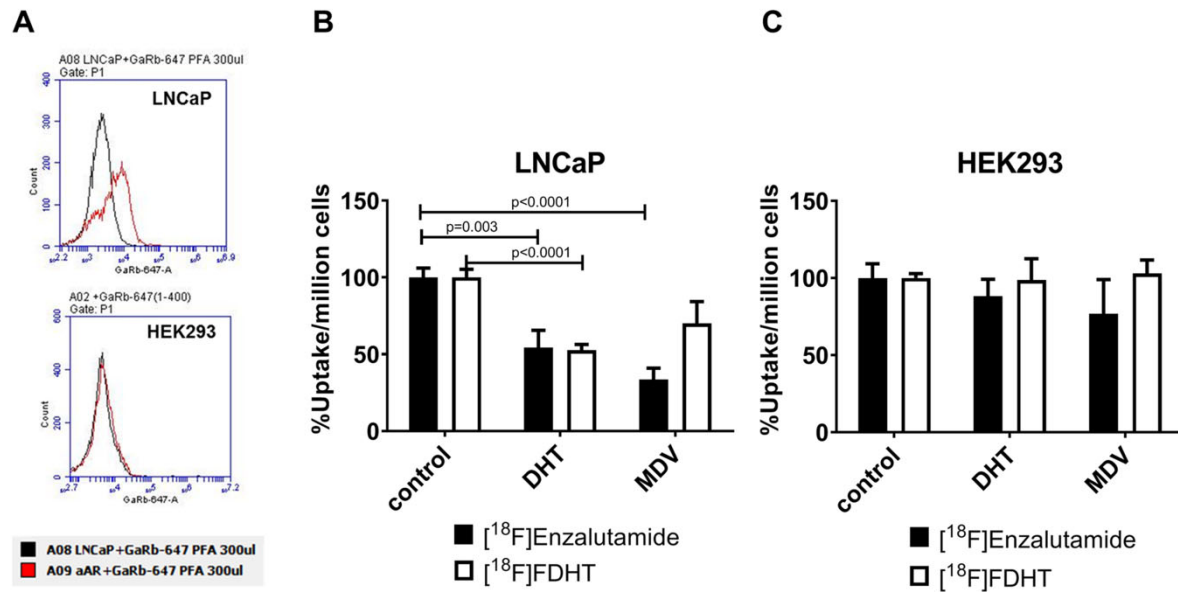
Figure 2. Scheme of the radiosynthesis of ^{18}F-FDHT.

Figure 3. **A)** FACS analysis of AR expression in different cell lines. Cell-associated radioactivity of ^{18}F-enzalutamide and ^{18}F-FDHT in **B)** LNCaP (AR+) and **C)** HEK293 (AR-) cells in the absence/presence of unlabeled DHT (1nM) or MDV (1nM). Results are expressed as % radioactivity/million cells (mean ± standard deviation).
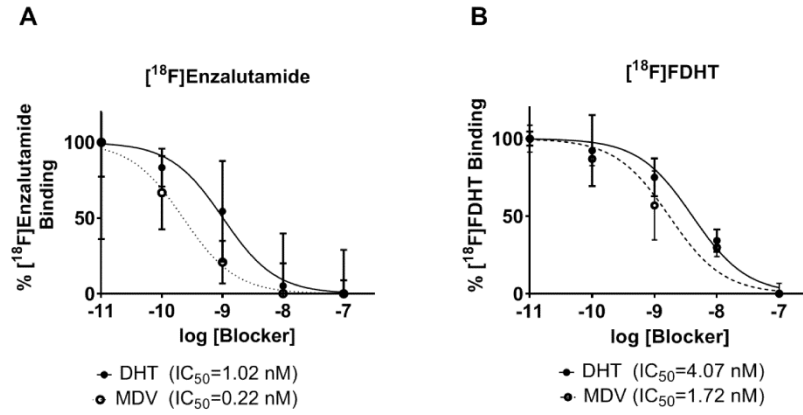
Figure 4. In-vitro competitive AR binding assay of **A)** ^{18}F-enzalutamide and **B)** ^{18}F-FDHT in LNCaP cells, using enzalutamide (MDV) or dihydrotestosterone (DHT) as the competitor.
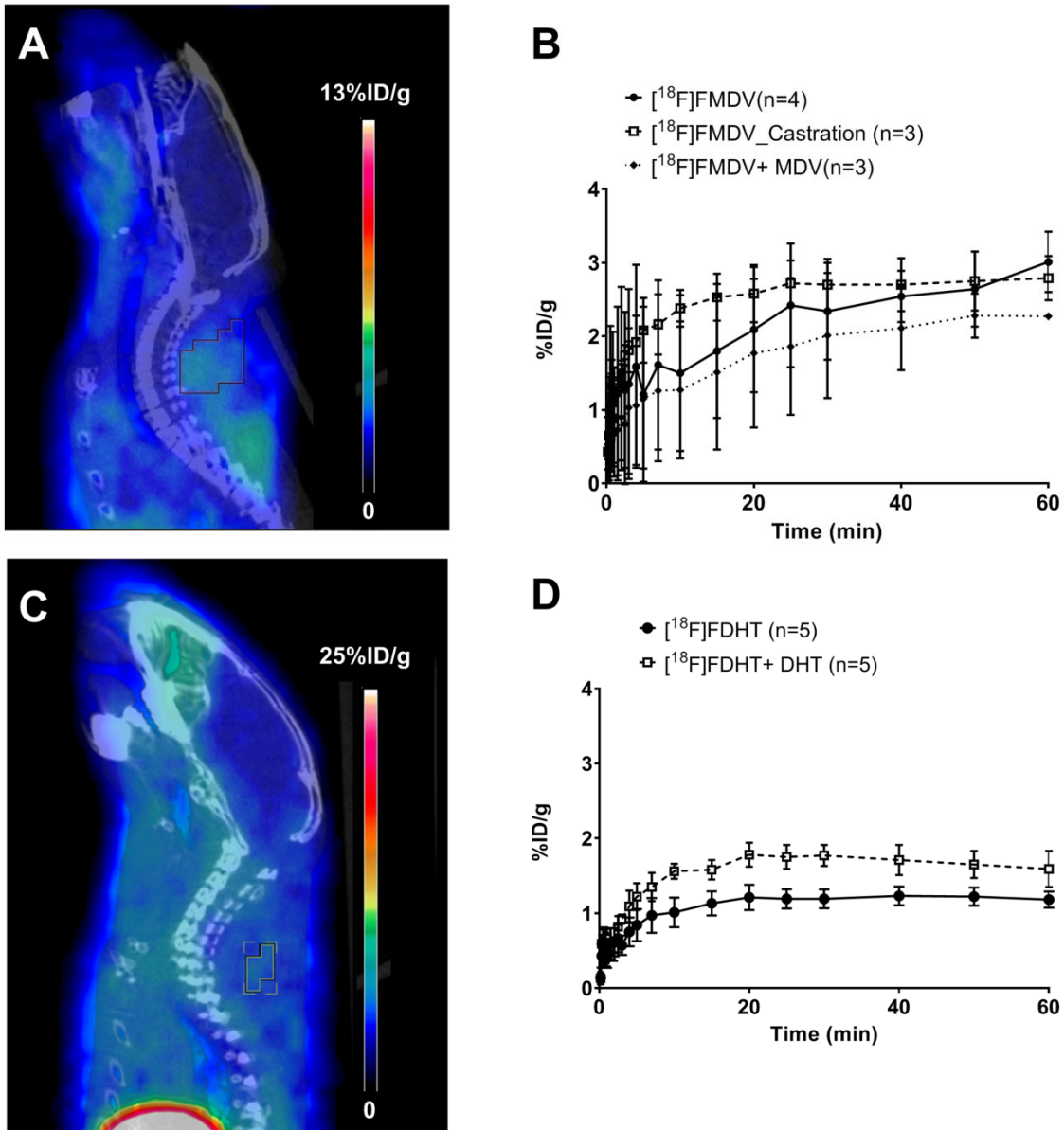
Figure 5. Sagittal microPET/CT fusion images of a mouse bearing a LNCaP xenograft (delineated) injected with **A)** [18F]enzalutamide (14±7 MBq) or **C)** 18F-FDHT (9±4 MBq). Time activity curves of the tumor uptake (%ID/g) of **B)** 18F-enzalutamide or **D)** 18F-FDHT in LNCaP xenografts.

Table 1 – Biodistribution 1 h after intravenous injection of ^{18}F-enzalutamide or ^{18}F-FDHT in castrated and non-castrated mice bearing an LNCaP tumor. Competition studies were performed in non-castrated mice by co-injection of the tracer with either enzalutamide (0.06 mg/g animal) or DHT(0.04 mg/g animal). Data are expressed as %ID/g (mean ± standard deviation). Statistically significant differences between treated and control animals (castrated vs. non-castrated and AR blocker vs. vehicle) are indicated by asterisks: * for p<0.05.
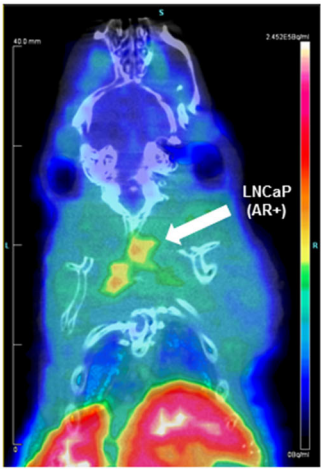
Organ	^{18}F-enzalutamide (n=5) [a]	^{18}F-enzalutamide + Castration (n=3) [b]	^{18}F-enzalutamide + enzalutamide (0.13 µmol/g animal) (n=5) [a]	^{18}F-FDHT (n=5) [a]	^{18}F-FDHT +DHT (0.13 µmol/g animal) (n=5) [a]
Bone	3.01± 0.63	2.41± 0.12	0.95± 0.14*	3.04± 0.54	3.18±1.62
Brain	1.62±0.71	1.66±0.32	1.75±0.43	0.56±0.07	0.96±0.54
Brown Fat	14.64±5.60	12.85±2.44	15.89±7.81	2.17±0.70	1.24±0.35
Heart	4.80±0.52	5.82±1.01	4.44±0.52	2.28±0.34	2.70±1.30
Kidney	6.51±3.01	6.37±1.00	5.21±0.52	5.33±0.84	4.95±1.86
Liver	14.17±0.98	12.76±1.67	8.36±1.27*	22.76±3.16	9.91±4.48*
Lung	3.48±0.44	5.03±1.59	3.34±0.29	2.01±0.37	2.50±1.30
Muscle	2.61±0.51	2.79±0.16	2.39±0.83	1.77±0.38	2.78±2.47
Plasma	0.89±0.41	0.61±0.23	1.40±1.25	2.58±0.48	2.24±1.26
Red blood cells	2.09±0.64	2.24±0.27	2.52±1.48	2.49±0.54	3.39±2.51
Spleen	4.66±1.25	5.26±1.48	1.89±0.62*	1.93±0.30	1.92±0.87
Prostate	3.37±1.15	6.15±0.51*	4.37±1.41	2.72±0.80	2.39±1.40
Urine	0.57±0.29	0.15±0.06	0.14±0.06*	19.84±6.36	6.53±7.72
Tumor	5.74±1.31[d]	4.45±2.65	3.64±0.26[c]*	1.63±0.22	1.59±0.82[d]

[a] 1 animal showed extravasation during tracer injection. [b] 3 animal showed extravasation during tracer injection. [c] 2 animals did not develop a tumor. [d] 1animal did not develop a tumor.
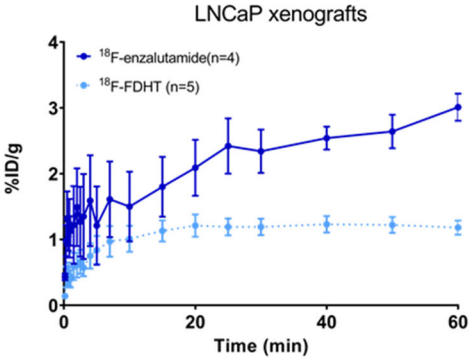
GRAPHICAL ABSTRACT
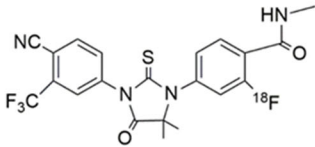
^{18}F-enzalutamide

^{18}F-enzalutamide

Synthesis and evaluation of ^{18}F-enzalutamide, a new radioligand for PET Imaging of Androgen Receptors: A comparison with 16β-^{18}F-fluoro-5α-dihydrotestosterone

Inês F. Antunes[1*], Rutger J. Dost[2], Hilde D. Hoving[2], Aren van Waarde[1], Rudi A.J.O Dierckx[1], Douwe F. Samplonius[3], W. Helfrich[3], Philip H. Elsinga[1], Erik F.J. de Vries[1] and Igle J. de Jong[2]

1. Dept. of Nuclear Medicine and Molecular Imaging, University Medical Center Groningen, University of Groningen, Groningen, The Netherlands

2. Dept. of Urology, University Medical Centre Groningen, University of Groningen, Groningen, The Netherlands

3. Surgical Research Laboratory, University Medical Centre Groningen, University of Groningen, Groningen, The Netherlands

*i.farinha.antunes@umcg.nl

TABLE OF CONTENTS

SUPPLEMENTAL MATERIAL

General Information

Reagents and solvents were obtained from commercial suppliers (Aldrich, Fluka, Sigma, Merck and Activate-Scientific) and used without further purification. Flash chromatography was performed on silica gel 60 (0.040-0.063, Merck). All reactions were monitored by thin layer chromatography on Merck F-254 silica gel plates. Detection of the compounds on the TLC plates was performed with UV light (254 nm). High-resolution mass spectra (HRMS) were obtained using a Xevo QTof UPLC/MS/MS system (Waters, Milford, USA), mounted with ACQUITY UPLC BEH C18 1.7 µm column, H_2O/CH_3CN + 0.1% HCOOH as eluent at a flow of 0.6 mL/min, ESI positive mode. Ultra-high performance liquid chromatography (UPLC) spectra were acquired using a Waters Acquity UPLC integrated system coupled to a Berthold Technologies Flowstar LB 513 radio flow detector. UPLC data was processed with Waters Empower 2 software. ^{1}H-NMR and ^{13}C-NMR spectra were recorded on a Varian 500 MHz apparatus. Chemical shifts were determined relative to the signal of the solvent, converted to the tetramethylsilane (TMS) scale and expressed in δ units (ppm) downfield from TMS. Coupling constants were reported in Hertz (Hz). Splitting patterns are defined as s (singlet), d (doublet), dd (double-doublet), t (triplet), dt (double-triplet) or m (multiplet). A glucose, magnesium, and calcium-containing buffer solution (GMC-PBS) was prepared by adding 5.6 mM D-glucose, 0.49 mM $MgCl_2$, and 0.68 mM $CaCl_2$ to 100 mL phosphate-buffered saline (PBS).

Chemistry

N-Methyl-2-nitro-4-bromobenzamide (1) (Supplemental figure 1). Thionyl chloride (350µL, 5.18 mmol) was slowly added to a solution of 2-nitro-4-bromobenzoic acid (1.1 g, 4.5 mmol) in EtOAc (6.5 mL, 4.5 mmol) and DMF (7 µL, 0.09 mmol) under nitrogen atmosphere. The mixture was then heated to 60-68 °C for 3.5 h, followed by 1

h reaction at 70-72 °C. The mixture was cooled down to 2-10 °C. A mixture of aqueous methylamine (40%, 1.6 ml, 22.5 mmol) in EtOAc was then slowly added to the vial and allowed to react for 50 minutes. Ethyl acetate (50mL) was added and the mixture washed with brine (3x25mL). The organic layers were dried with sodium sulfate, filtered and concentrated. The final product was left stirring overnight in a solution of heptane/EtOAc (2:1), filtered and dried to yield compound **1** (0.53 g, 45%) as a yellow solid.

¹H NMR (500 MHz, CDCl₃) δ 8.21 (d, J = 1.8 Hz, 1H), 7.82 (dd, J = 8.1, 1.9 Hz, 1H), 7.42 (d, J = 8.1, 1H), 5.90 (s, 1H), 3.04 (d, J = 4.9 Hz, 3H)

HRMS-ESI: m/z 261.1 [M+1]$^{+}$.

2-(3-nitro-4-(methylcarbamoyl)phenylamino)-2-methylpropanoic acid (2). Compound 1 (0.42g, 1.6 mmol), aminoisobutyric acid (0.25 g, 2.4 mmol), potassium carbonate (0.56, 4.0 mmol), copper chloride 99% (0.032g,0.32 mmol), DMF (3mL) and water (90 µL) were added to a flask and the reaction mixture was stirred at room temperature for 5 min. Then 2-acetylcyclohexanone (42 µL, 0.32 mmol) was added to the mixture and allowed to react at 105 °C for 18 h under a nitrogen atmosphere. After the mixture was cooled to room temperature, the product was extracted with ethyl acetate and water. The lower aqueous layer was acidified with 1 M citric acid to pH 4.0 and the product extracted with ethyl acetate, dried with NaSO₄, filtered and concentrated under vacuum to yield 0.26 g (57% yield) of the final product as brown crystals.

¹H NMR (500 MHz, CDCl₃) δ 8.23 (d, J = 1.8 Hz, 1H), 7.83 (dd, J = 8.1, 1.8 Hz, 1H), 7.43 (d, J = 8.1 Hz, 1H), 5.79 (s, 1H), 3.06 (d, J = 4.9 Hz, 3H), 1.57 (s, 6H).

HRMS-ESI: m/z 282.1 [M+1]$^{+}$.

Methyl 2-(3-nitro-4-(methylcarbamoyl)phenylamino)-2-methylpropanoate (3). Methyl iodide (79 µL) was added in one portion to a mixture of compound 2 (0.26 g,

0.93 mmol), potassium carbonate (0.17 g, 1.3 mmol) in DMF (2 mL) and water (5 μL) and allowed to react at 60 °C for 2 h until the reaction was complete. The solvent was evaporated, MeOH and ether were added and the mixture was left overnight at 4 °C, resulting in the formation of 185 mg (55 %) of crystalized pure product.

1H NMR (500 MHz, CDCl3) δ 7.29 (s, J = 3.2 Hz, 1H), 7.20 – 7.15 (m, 1H), 6.87 – 6.74 (m, J = 7.8 Hz, 1H), 6.05 – 5.95 (m, 1H), 3.78 (s, J = 10.4 Hz, 3H), 3.00 (d, J = 4.8 Hz, 3H), 1.64 (s, 6H)

HRMS-ESI: m/z 296.1 [M+1]$^+$.

4-(3-(4-cyano-3-(trifluoromethyl)phenyl)-5,5-dimethyl-4-oxo-2-thioxoimidazolidin-1-yl)-2-nitro-N-methylbenzamide (precursor). A solution of compound 3 (0.15g, 0.51 mmol) and 2-(trifluoromethyl)-4-isothiocyanatobenzonitrile (0.26 g, 1.1 mmol) in DMSO (200 μL) and ethyl acetate (2 mL) was heated at 85 °C for 21 h. Once the reaction mixture was cooled down to room temperature, the mixture was diluted with water and extracted with ethyl acetate. The organic layer was dried with NaSO4, filtered and concentrated under reduced pressure. The product was purified by silica gel chromatography (n-hexane/ethyl acetate= 3:1) to yield 35 mg (14%) of a yellow solid.

1H NMR (500 MHz, CDCl3) δ 8.14 – 7.92 (m, 3H), 7.87 – 7.81 (m, 1H), 7.76 – 7.60 (m, 2H), 6.40 (dd, J = 9.7, 5.0 Hz, 1H), 3.05 (d, J = 5.0 Hz, 3H), 1.72 – 1.51 (m, 6H)

13C NMR (500 MHz, DMSO) δ 23.3 (2C), 26.6, 67.2, 109.3, 115.4, 126.5, 128.34, 133.6, 134.4 (2C), 135.4, 136.7 (2C), 137.4, 138.3, 147.7, 165.6, 175, 180.8

HRMS-ESI: *m/z* 492.1[M+1]$^+$

In-vitro

Stability of ^{18}F-enzalutamide. Formulated ^{18}F-enzalutamide in 16% aqueous ethanol (1 mL) was stored at room temperature for 60 min. The solution was reanalyzed for the presence of degradation products by UPLC (retention time: ^{18}F-fluoride =0.5 min, ^{18}F-enzalutamide= 3.96 min).

Distribution coefficient (Log $D_{7.4}$). To determine the Log $D_{7.4}$ of ^{18}F-enzalutamide and ^{18}F-FDHT, an aliquot of 1 mL of purified [^{18}F-enzalutamide or ^{18}F-FDHT solution was added to a mixture of n-octanol/PBS (3ml/3ml) at pH 7.4. The tubes were vortexed at room temperature for 1 min, followed by 30 min of shaking in a water bath at 37 $^{\circ}$C. Aliquots of 0.5 mL were drawn from the n-octanol and aqueous phase, respectively, and the radioactivity was counted using an automated gamma counter (Compugamma, LKB Wallac). The experiments were performed in triplicate.

Cells and culture conditions. The LNCaP and Hek293 cell lines were kindly provided by the Surgical Research Laboratory of the UMCG. Cells were cultured in RPMI supplemented with 10% fetal calf serum in a humidified atmosphere with 5% CO_2 at 37 $^{\circ}$C.

Androgen receptor expression. 10^5 LNCaP or HEK293 cells were fixed with 3% paraformaldehyde (PFA) for 10 min at room temperature, followed by washing with phosphate-buffered saline (PBS). Next, cells were incubated with anti-Androgen Receptor antibody (clone D6F11 dilution1:400, Cell Signaling) at 4°C for 30 min and subsequently washed twice with PBS. Cells were then stained with Alexa Fluor 647 goat anti-Rabbit IgG (Invitrogen, dilution1:200) at 4°C for 30 min and subsequently washed twice with PBS. Fluorescent intensity of the cells was analyzed on an Accurci C6 flow cytometer (Becton Dickinson).

In-vitro competitive AR binding assay. For competition assays, LNCaP [AR(+)] and Hek293 [AR(-)] cells were plated in triplicate in a 24-well plate at a density of 10^5

cells per well, one day before the assay. The medium was discarded and the cells were washed twice with PBS and 0.4 mL of PBS-GMC with 0.5% HSA buffer per well was added. Just before the addition of the PET tracer, the medium was discarded once more. Cells were washed twice with warm PBS and 0.5 mL of PBS-GMC with 0.5% HSA buffer was added, followed by the addition of 50 µL ^{18}F-enzalutamide or ^{18}F-FDHT in the absence or presence of different concentrations of DHT or enzalutamide. After the cells were incubated for 60 min, the medium was discarded. The cells were washed with cold PBS (3×0.5 mL/well), harvested with trypsin (100 µL) and resuspended in 900 µL of DMEM. The cell suspensions were collected separately for each well and the radioactivity was measured using a gamma counter. A 50 µL sample of the suspension was mixed with 50 µL of trypan blue and used for cell counting. Cell numbers were manually determined, using a phase-contrast microscope (Olympus), a Burker bright-line chamber (depth 0.1 mm: 0.0025-mm^2 squares) and a hand-tally counter. Cellular uptake of radioactivity was corrected for the number of cells.
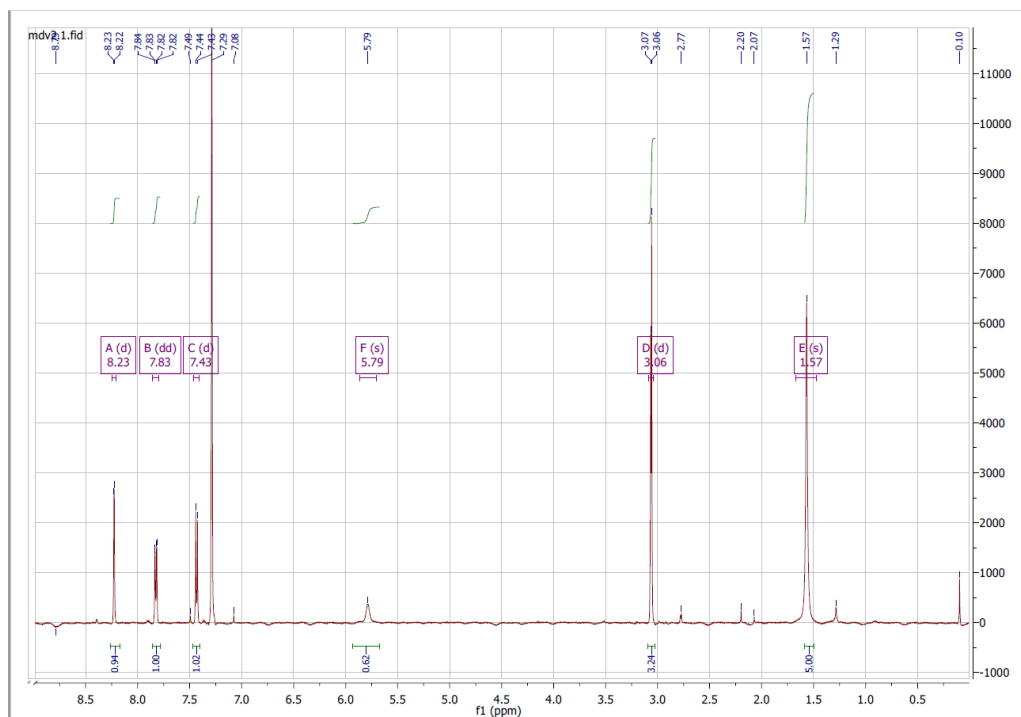
Characterization of Compounds

N-Methyl-2-nitro-4-bromobenzamide (1)-1H NMR
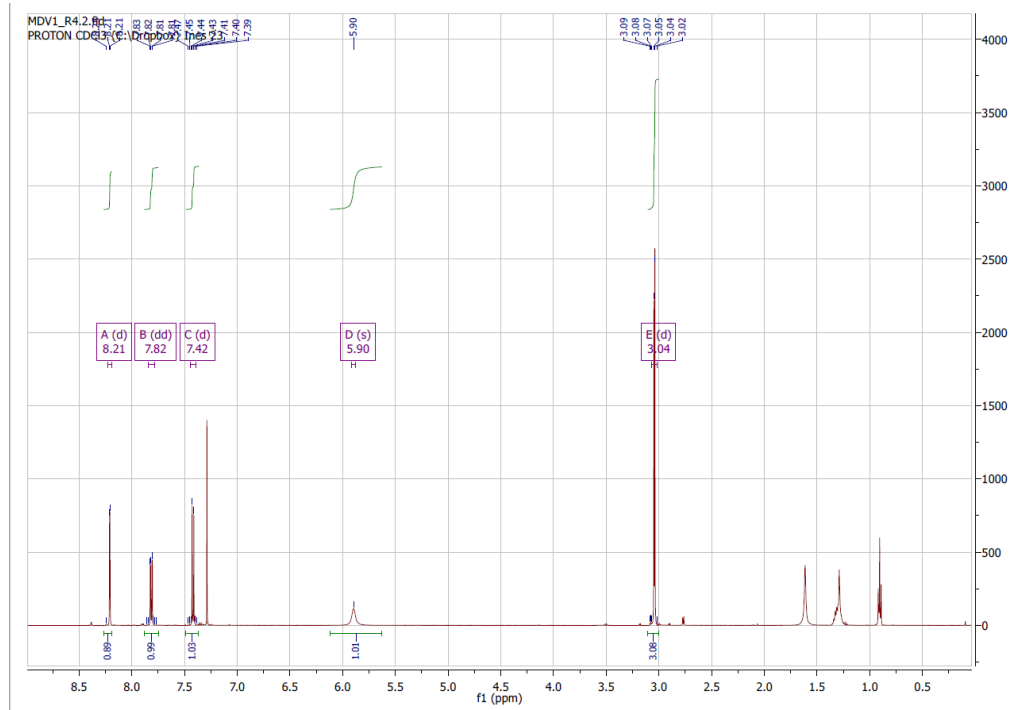
2-(3-nitro-4-(methylcarbamoyl)phenylamino)-2-methylpropanoic   acid   (2)   -1H
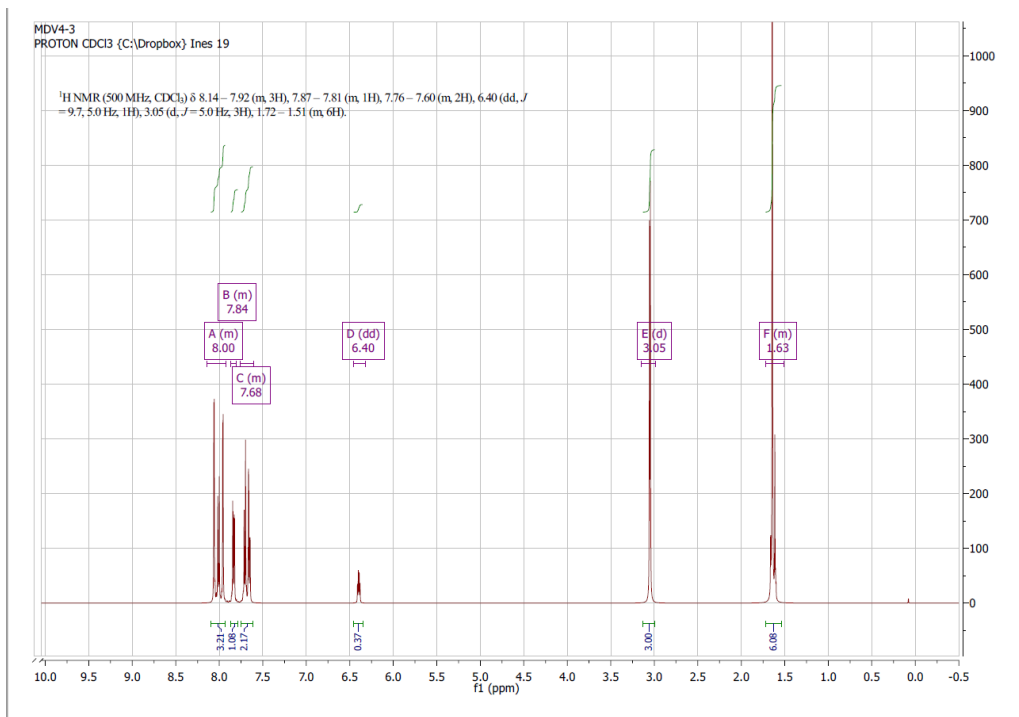
NMR

Methyl 2-(3-nitro-4-(methylcarbamoyl)phenylamino)-2-methylpropanoate (3) -1H
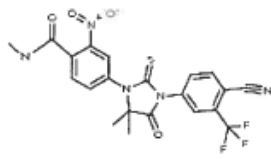
NMR

4-(3-(4-cyano-3-(trifluoromethyl)phenyl)-5,5-dimethyl-4-oxo-2-thioxoimidazolidin-1-yl)-2-nitro-N-methylbenzamide (precursor) -^{1}H, ^{13}C NMR and HRMS-ESI
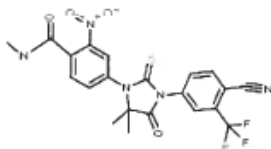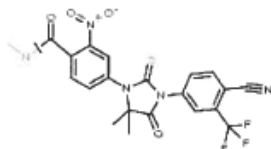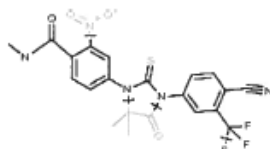

MDV4-3
PROTON CDCl3 {C:\Dropbox} Ines 19

^{1}H NMR (500 MHz, CDCl$_3$) δ 8.14 – 7.92 (m, 3H), 7.87 – 7.81 (m, 1H), 7.76 – 7.60 (m, 2H), 6.40 (dd, J = 9.7, 5.0 Hz, 1H), 3.05 (d, J = 5.0 Hz, 3H), 1.72 – 1.51 (m, 6H).

MDV 4-3
C13 DMSO {C:\NMR data\PET} MartaW 31

Report

Input:

|		
	ID (job)	75
	Mass (Da)	491.0875
	Formula	$C_{21}H_{16}N_5O_4F_3S$
	DBE	15

Experiment:

Product ion(s) (Da)	321.0245 323.0226 353.0506 354.0536 355.0486 356.0518 461.0540 492.0961 600.1326 602.1312 +/- 0.01 in positive mode, structure filter off
DBE	-10 to 50
Electron count	both
Maximum H deficit	6
Fragment number of bonds	4
Scoring	aromatic: 6, multiple: 4, ring: 2, phenyl: 8, other: 1 H-deficit: 0, hetero modifier: 0.5, max score: 16
Order:	mass
Plot:	show ◉ hide ◎
Files:	CSV

Results:

492.0961 ⌐+ (+1H)	461.0540 ⌐+ (+0H)	355.0486 ⌐+ (-1H)
492.0953 (+0.8.mDa) $C_{21}H_{17}N_5O_4F_3S$ (-none)	461.0531 (+0.9.mDa) (S:0.5, B:1) $C_{20}H_{12}N_4O_4F_3S$ (-CH$_5$N)	355.0465 (+2.1.mDa) (S:12.5, B:4) $C_{17}H_9N_4OF_2S$ (-C$_4$H$_8$NO$_3$F)

20140319_03 492 (1.889) Cm (473:492-239:342) - 1: TOF MS ES+
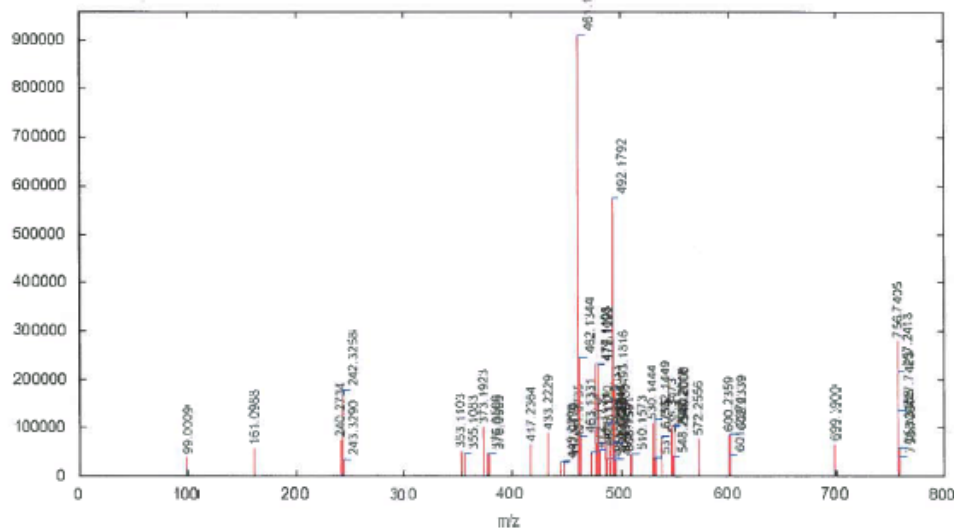
Characterization of the precursor and Enzalutamide by radio-UPLC

Radio-UPLC profile of the Precursor

Sample Name: precursor test
Sample Type: Unknown
Vial: 2:A,8
Injection #: 1
Injection Volume: 10.00 ul
Run Time: 10.0 Minutes

Acquired By: Rolf
Sample Set Name:
Acq. Method Set: MDV_ms
Processing Method MDV_254_pm
Channel Name: ACQUITY TUV ChA
Proc. Chnl. Descr.: ACQUITY TUV ChA 254nm

Chromatogram

Channel ACQUITY TUV ChA
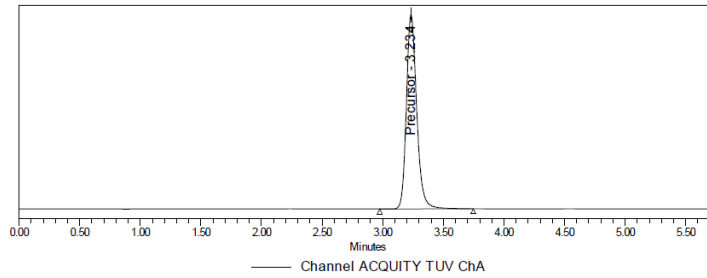
Components table
Channel: ACQUITY TUV ChA

	Peak Name	RT	Height	Area	% Area	Amount	Units	volume_ml	activity_MBq	time_EOS	SA_GBqmmol	Channel
1	Impurities	1.000										ACQUITY TUV ChA
2	MDV	3.800										ACQUITY TUV ChA
3	Precursor	3.234	2291490	13550394	100.00							ACQUITY TUV ChA

Radio-UPLC profile of the Enzalutamide

Sample Name: MDV std
Sample Type: Unknown
Vial: 1:B,1
Injection #: 1
Injection Volume: 10.00 ul
Run Time: 10.0 Minutes

Acquired By: Rolf
Sample Set Name:
Acq. Method Set: MDV_ms
Processing Method MDV_254_pm
Channel Name: ACQUITY TUV ChA
Proc. Chnl. Descr.: ACQUITY TUV ChA 254nm

Chromatogram

Channel ACQUITY TUV ChA
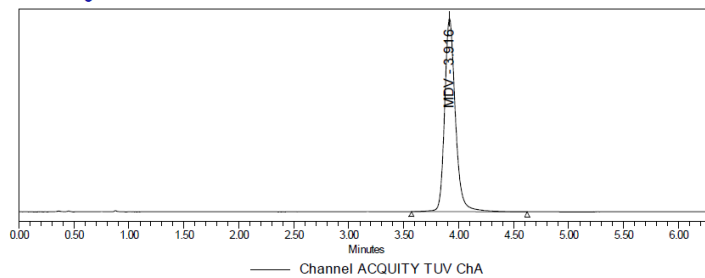
Components table
Channel: ACQUITY TUV ChA

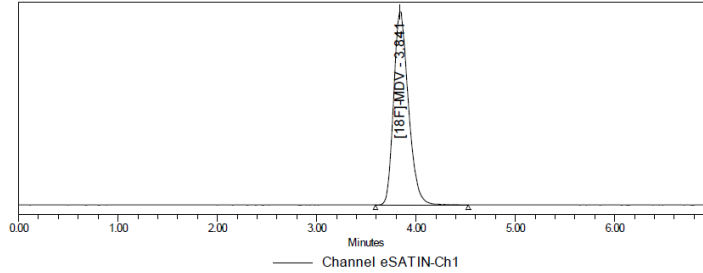|	Peak Name	RT	Height	Area	% Area	Amount	Units	volume_ml	activity_MBq	time_EOS	SA_GBqmmol	Channel
1	Impurities	1.000										ACQUITY TUV ChA
2	MDV	3.916	127852	870141	100.00	15.988						ACQUITY TUV ChA

Characterization of ^{18}F- Enzalutamide by radio-UPLC

Radio-UPLC profile of the ^{18}F-Enzalutamide

Sample Name: MDV 14-07
Sample Type: Unknown
Vial: 1:A,4
Injection #: 1
Injection Volume: 10.00 ul
Run Time: 7.0 Minutes

Acquired By: Rolf
Sample Set Name:
Acq. Method Set: MDV_ms
Processing Method MDV_act_pm
Channel Name: eSATIN-Ch1
Proc. Chnl. Descr.: Activity

Chromatogram

— Channel eSATIN-Ch1

Components table
Channel: eSATIN-Ch1

	Peak Name	RT	Height	Area	% Area	Amount	Units	volume_ml	activity_MBq	time_EOS	SA_GBqmmol	Channel
1	[18F]F-	0.500						6	258	15:49		eSATIN-Ch1
2	[18F]-MDV	3.841	320413	3288599	100.00			6	258	15:49		eSATIN-Ch1

Radio-UPLC profile of the ^{18}F-Enzalutamide with UV

Sample Name: MDV 14-07
Sample Type: Unknown
Vial: 1:A,4
Injection #: 1
Injection Volume: 10,00 ul
Run Time: 7,0 Minutes

Acquired By: Rolf
Sample Set Name:
Acq. Method Set: MDV_ms
Processing Method MDV_254_pm, MDV_act_pr
Channel Name: eSATIN-Ch1, ACQUITY TUV
Proc. Chnl. Descr.: ACQUITY TUV ChA 254nm,

Chromatogram

— Channel eSATIN-Ch1
— Channel ACQUITY TUV ChA
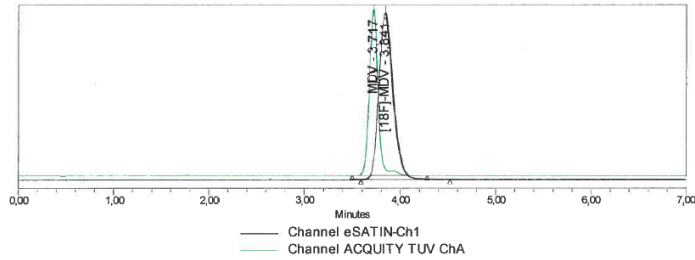
Components table
Channel: ACQUITY TUV ChA

	Peak Name	RT	Height	Area	% Area	Amount	Units	volume_ml	activity_MBq	time_EOS	SA_GBqmmol	Channel
1	Impurities	1,000						6	258	15:49		ACQUITY TUV ChA
2	Precursor	1,500						6	258	15:49		ACQUITY TUV ChA
3	MDV	3,717	182643	1194075	100,00	21,940		6	258	15:49	726	ACQUITY TUV ChA

Components table
Channel: eSATIN-Ch1

	Peak Name	RT	Height	Area	% Area	Amount	Units	volume_ml	activity_MBq	time_EOS	SA_GBqmmol	Channel
1	[18F]F-	0,500						6	258	15:49		eSATIN-Ch1
2	[18F]-MDV	3,841	320413	3288599	100,00			6	258	15:49		eSATIN-Ch1

Supplemental Figures
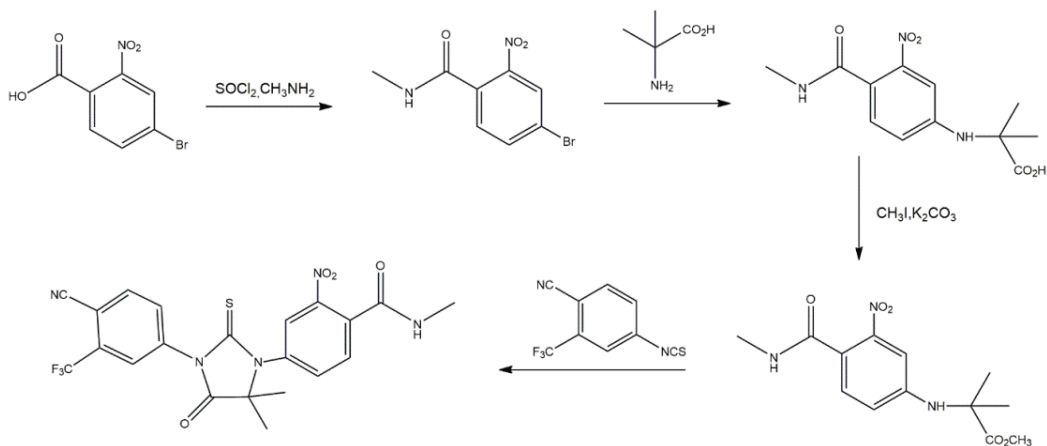
Supplemental Figure 1. Synthesis of the Nitro-precursor
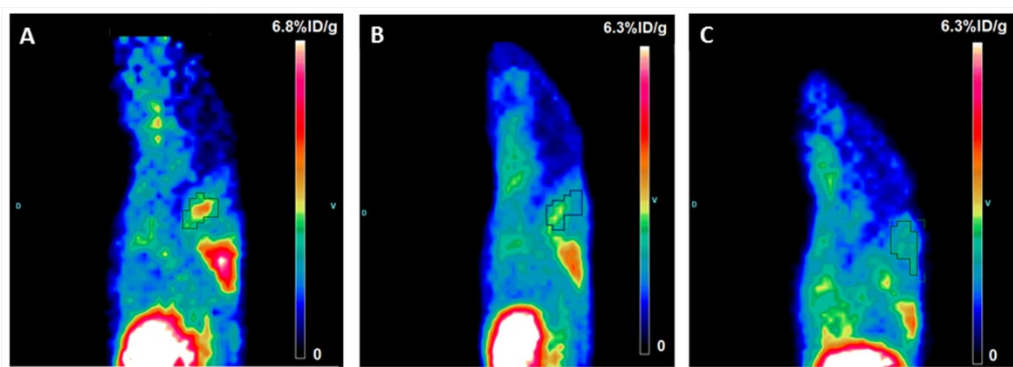
Supplemental Figure 2. Sagittal microPET images of: **A)** a non-castrated or **B)** castrated mouse bearing a LNCaP xenograft (delineated) injected with ^{18}F-enzalutamide and **C)** a non-castrated mouse bearing a LNCaP xenograft (delineated) injected with ^{18}F-enzalutamide and cold enzalutamide (0.13 μmol/g animal).